Progress In Electromagnetics Research B, Vol. 90, 151–166, 2021

Lorentz Force Contribution to Thunderstorm's Electrical Characteristics

Babak Sadeghi[1, *], Amir A. Shayegani Akmal[1], and Farahnaz Taghavi[2]

Abstract—In this paper, the exerted electric and geomagnetic forces on the electrified hydrometeors in thunderclouds are compared. The parameters of geomagnetic field are acquired from International Geomagnetic Reference Field (IGRF) model. First, the calculations showed that the magnitude of the electric force exerted on a charged hydrometeor dominated the magnitude of the geomagnetic force in troposphere. These results revealed the significance of electric force in the formation of thunderclouds' charge structure. Moreover, as the electric field increases in thunderstorm conditions, (regarding the dependence of the induction mechanism of cloud electrification to the intensity of the electric field), the increased electric field strengthens the induction mechanism of cloud electrification and influences the electrical properties of thunderstorm. Second, using satellite-based/ground-based data and reports, an inverse relation has been revealed between the total geomagnetic field and the mean annual lightning activity in most of the hot spots on the Earth. Moreover, a comparison between the global annual thunder days' map and the map of global total geomagnetic field showed an inverse relation between these two maps. Furthermore, regarding the horizontal and vertical correlation coefficient matrices of the geomagnetic field and the global mean annual lightning activity (in the global tropics and subtropics), approximately in latitudes and longitudes with high lightning density, the reverse relation between the average annual lightning activity and the total geomagnetic field is stronger.

1. INTRODUCTION

There exists a vertical fair weather electric field (around 10^2 V m^{-1}) near the Earth's surface which results from the negative charges on the surface of the Earth and the positive charges in the air prior to the lightning initiation. The electric field in the thundercloud rises, but this field is much smaller than the conventional breakdown threshold field of the air which is 3.2×10^6 V m^{-1} at ground pressure [1–4]. The separation of charges in the thundercloud may eventually produce an electric field that becomes so large (around $3 \times 10^5 \sim 4 \times 10^5$ V m^{-1}) that it could initiate the lightning stroke [5]. One fact agreed by most of researchers [6–12] is the contribution of intense lightning discharges to the global electric circuit (GEC). The substantial role of the lightning and thunderstorm in GEC would justify the need to investigate the charge structure of thunderclouds.

Researchers pointed out that there could be other unknown methods for describing the causes of cloud electrification, electric field development, and lightning initiation [1]. The effects of the electric and magnetic forces might be two of the important methods which may take part in electrical properties of thunderclouds.

The goal of this study is to compare the electric and magnetic forces exerted on the electrified hydrometeors in thunderclouds. This study is structured as follows. First, the data and methods are presented. Second, we discuss the results. Ultimately, in the final section, we provide a concise conclusion of the study.

Received 10 December 2020, Accepted 7 January 2021, Scheduled 18 January 2021
* Corresponding author: Babak Sadeghi (babaksadeghi14@ut.ac.ir).
[1] Department of Electrical and Computer Engineering, University of Tehran, Iran. [2] Department of Space Physics, Institute of Geophysics, University of Tehran, Iran.

2. DATA AND METHOD

2.1. Effects of the Lorentz Force on the Charge Structure of Thunderstorms

The Lorentz force (the exerted force on a moving charged particle due to the combined electric and magnetic fields) may be a possible contributor to the formation of tornados [13]. Regarding the Lorentz force equation, after hydrometeors' electrification (by each process of cloud electrification) the moving positive and negative charges could be influenced by both of the electric and magnetic forces

$$\vec{F} = q \cdot (\vec{V} \times \vec{B}) + q \cdot \vec{E} \tag{1}$$

where $\vec{F}, q, \vec{V}, \vec{B}$ and $\vec{E}$ stand for the Lorentz force, hydrometeor's charge, velocity of hydrometeor, geomagnetic field, and atmospheric electric field, respectively.

The charged areas of the cloud tend to place between 3 km and 10 km above the Earth's surface [14]. Water droplets and ice crystals in the clouds are thought to be the charge carriers which produce huge electric fields necessary for lightning initiation [13]. In thunderstorms, small particles (1–2 mm in diameter) have often been observed to carry charges of a few hundred Pico-coulombs [5, 15].

In this subsection of the study, the geomagnetic field components are extracted from IGRF model in order to investigate the geomagnetic force acting on an electrified hydrometeor in thunderstorm. The IGRF model is a standard mathematical description of the geomagnetic field which is created by fitting parameters of a mathematical model of the magnetic field to the measured magnetic field data from surveys, observatories, and satellites across the globe. The IGRF has been produced and updated under the direction of the International Association of Geomagnetism and Aeronomy (IAGA) since 1965.

The IGRF function is valid between the heights of −1 km (1 km below the Earth's surface) and 600 km (above the Earth's surface); this model also contains the data of the geomagnetic field in different years (from 1900). The geocentric components of the geomagnetic field could be obtained from IGRF model [16]. In this study, we select the Cartesian coordinate system (in which x, y, and z represent northward, eastward, and radially inwards directions, respectively).

The geomagnetic field vector could be described by the orthogonal components: B_x (northward intensity), B_y (eastward intensity), and B_z (downward intensity). The horizontal intensity (B_H) is described as the net of B_x and B_y ($B_H = \sqrt{B_x^2 + B_y^2}$). The total intensity of the geomagnetic field (B_T) is the net of B_x, B_y, and B_z ($B_T = \sqrt{B_x^2 + B_y^2 + B_z^2} = \sqrt{B_H^2 + B_z^2}$). Inclination ($I$) is the angle between the horizontal plane and the geomagnetic field vector, measured positive downwards ($I = \tan^{-1}(B_z/B_H)$). Declination (D) is the horizontal angle between the true north and the field vector, measured positive eastwards ($D = \tan^{-1}(B_y/B_x)$) [17]. Using IGRF model, both of the Inclination and Declination of the geomagnetic field could be obtained in degrees.

Some observational results [18, 19] are clues which specify the significance of the hydrometeors' velocity in the formation of the thunderclouds' charge structure. A strong correlation between the hydrometeors' velocity and the lightning activity is reported by some researchers [20–23].

Observations of cloud electrification showed that both the intensity and direction of the hydrometeor's velocity crucially impact the thundercloud's electrical properties. Therefore, it could be useful to investigate the role of the hydrometeors' velocity in thundercloud's electrical properties considering the geomagnetic field as a medium regarding the magnetic term of the Lorentz force equation (the first term of Eq. (1)).

In this study, it is supposed that the electrified hydrometeor's velocity has three components (V_x, V_y, and V_z which symbolize the northward, eastward, and downward components, respectively). The signs of the updraft motion and upward magnetic force are considered negative (−). Based on Eq. (2), the geomagnetic force (emanated from both of the geomagnetic field and the velocity of the electrified hydrometeors) has three components (based on the magnetic term of the Lorentz force equation, in Cartesian coordinate, the geomagnetic force could be as follows):

$$\begin{cases} F_x = q(V_y B_z - V_z B_y), & Northward\ Magnetic\ Force \\ F_y = q(V_z B_x - V_x B_z), & Eastward\ Magnetic\ Force \\ F_z = q(V_x B_y - V_y B_x), & Downward\ Magnetic\ Force \end{cases} \tag{2}$$

The amount of the geomagnetic field's components (B_x, B_y, B_z), which could be acquired from IGRF model, depends on the location of the hydrometeor in troposphere. Different components of the velocity (V_x, V_y, V_z) with regard to the geomagnetic field lead to geomagnetic force $(F_x, F_y, F_z))$; F_T stands for the total geomagnetic force which is the net of the northward, eastward, and downward components of the geomagnetic force ($F_T = \sqrt{F_x^2 + F_y^2 + F_z^2}$).

2.2. Effects of the Electric Field on the Electrical Properties of Thunderstorms

The diurnal cycle of the atmospheric potential gradient (the vertical electric field) had been measured on the research ship Carnegie in a series of cruises between 1909 and 1929 [24]. The diurnal variation in the atmospheric potential gradient is correlated with the diurnal variation in the global thunderstorm activity [25].

There is a good correlation between the magnitude of the current measured on fair-weather days and the presence of the jet stream. This relation indicates that a jet stream may carry a higher positive charge sufficient to enhance the typically positive fair-weather field under the area of the jet stream. A jet stream is often observed in the vicinity of strong thunderstorms or other stormy regions, including tornadoes [26].

Inductive mechanism of cloud electrification depends on the fair weather electric field to induce charges in hydrometeors so that particle rebounds can separate the opposite charges and strengthen the field [27]. Jet stream (which will give rise to fair weather electric field) could influence the inductive mechanism. As a result, it could be stated that the inductive mechanism will have a stronger effect on thunderstorm electrification (than when there is just fair weather electric field). Some observations were reported about the correlation between the atmospheric electrical activity and the jet stream.

In reference [28], it is indicated that abnormally strong electric fields should be considered in mathematical modeling (and analyzing the physical processes causing intensification) of tropical cyclones, hurricanes, and thunderstorms generating the tornadoes.

The electromagnetic phenomena play a significant role in many of the atmospheric processes. Electromagnetic forces could influence both generation (and maintenance) of the charged structure and the motion of tropical cyclones [29]. In reference [30], it is reported that the electrostatic forces could contribute to the warming of climate by increasing the concentration of large particles in atmospheric dust.

The goal of this study is to compare the electric and magnetic forces exerted on moving charged hydrometeors in thunderclouds. It is firstly required to have a rough perspective of the order of forces that act on electrified hydrometeors. In this study, the calculation of forces (force of gravity, electric force, and magnetic forces) is presented based on three amounts of observed charges on particles. Tiny charged water droplets (from 0.01 μm to 1 μm in diameter) with charges in the range of 9.8×10^{-18} to 2.5×10^{-14} Coulombs were considered in [13] while in this study, electrified hydrometeors are supposed to have radiuses from 10 μm to 1000 μm with charges of about 10^{-15} to 10^{-10} Coulombs.

2.3. Effects of the Geomagnetic Field on Electrical Properties of Thunderstorms

One of the aims of this study is to statistically investigate the influence of the geomagnetic field on thunder phenomena. Although because of the complexity of thunderstorms (and the rare in-situ measurements and observations), the underlying physical mechanisms could not be clearly identified, the role of the geomagnetic field in both inductive and non-inductive mechanisms of cloud electrification could be analyzed through conducting an evidence-based survey of the influences of the magnetic field on some features of the hydrometeors. Some researchers (e.g., [31–35]) investigated the experimental evidences for the impacts of the magnetic field on physical and chemical properties of water (viscosity, enthalpies, surface tension, amount of evaporated water, electric conductivity, dielectric constant, thermal conductivity, etc.).

The inductive mechanism of cloud electrification strongly depends on electrical conductivity of droplets [36]. On the other hand, regarding the aforementioned observations and experiments, the electrical conductivity of water will be affected with magnetic field application. Therefore, we propose

that the geomagnetic field could cause some changes in the inductive mechanism of cloud electrification through alteration of hydrometeors' electrical conductivity (which are moving in troposphere).

The main non-inductive mechanism of thunderstorms' electrification is the riming electrification (which mainly occurs during collisions between graupel particle and ice crystal) [37]. The factor that controls the sign of charge transfer during collisions is the relative diffusional growth rates (RDGR) of the interacting ice particle surfaces [36]. The crystal growth rate [38] depends on some parameters (e.g., the capacitance of water, the latent heat of sublimation, and the saturation vapor pressure). The capacitance of water depends on magnetic field (regarding the variations in dielectric permittivity of water after magnetic field treatment [33]). Moreover, the latent heat of sublimation varies with magnetic field application (because the hydrogen bonding of water molecules could be affected with magnetic field application [31]). Furthermore, the magnetic field could alter the saturation vapor pressure (as the surface tension and the saturation vapor pressure of water are correlated [32]). All in all, we propose that the geomagnetic field plays a role in determining the sign of charge transfer (in non-inductive collisional charge separation process), by changing the hydrometeor's microphysical parameters and affecting the RDGR of colliding particles, because at least three parameters of the crystal growth rate (capacitance, latent heat of sublimation, and saturation vapor pressure of water) could be affected with the geomagnetic field.

Scientists presented evidences about the relations between the geomagnetic field and the meteorological phenomena (e.g., pressure patterns). In reference [39], it is implied that in the upper troposphere, cyclones (anticyclones) prevail where the geomagnetic field is weak (strong). The intensity of the geomagnetic field could have a controlling effect on the meteorological pressure patterns in the troposphere [40]. In reference [41], it is reported that the spatial and temporal changes of the geomagnetic field may be associated with climatic changes (by controlling the precipitation of charged particles from the magnetosphere).

Some researchers studied the possible connection of the geomagnetic field with cloud formation, precipitation, temperature, and climate [42–44]. Their achievements showed that the cosmic rays generate electrically charged particles when they hit the atmosphere. These particles absorb the water molecules from the air and cause them to clump together until they condense into clouds. When (as a consequence of the stronger geomagnetic field) fewer cosmic rays hit the atmosphere, fewer clouds form, which causes warming.

There are several researches [45–50] indicating the relation between the cosmic rays and the atmospheric electricity (e.g., lightning frequency). Because the geomagnetic field protects the Earth from cosmic rays, there could be relations between the geomagnetic field and the atmospheric electricity.

Altogether, with regard to the aforementioned studies, there might be relationships between the geomagnetic field and both meteorological phenomena and atmospheric electricity. In fact, it could be concluded that as a consequence of the stronger geomagnetic field, fewer cosmic rays hit the atmosphere, and fewer clouds form, which causes lower risk of the lightning initiation. On the other hand, decrement of the geomagnetic field will result in penetration of more cosmic rays, and as a consequence the probability of the lightning initiation will be higher.

In general, we cannot ignore the magnetic field as an interface between electrical energy and mechanical energy. There are many devices which are designed with regard to the magnetic field as a medium (motors, generators, etc.). The important role of the magnetic field in different contexts triggers the idea that the geomagnetic field could affect the thunderstorms which are of main parts of the atmospheric electricity in GEC model.

Therefore in this study, some regions from five continents are selected in order to analyze the relation between the maps of the geomagnetic field (which are extracted from IGRF model) and the mean annual maps of both lightning activity and thunder day events (which are acquired from satellite-based/ground-based data and reports).

3. RESULTS AND DISCUSSION

In this study, three forces (geomagnetic force, electric force, and force of gravity) exerted on the moving electrified hydrometeors are calculated in order to analyze and compare the role of these forces in thunderstorms. Furthermore, the relations between the maps of the geomagnetic field and the mean

annual maps of both lightning activity and thunder day events are investigated.

3.1. Calculation of the Forces

In this subsection of the study, in order to investigate the effects of the electric and geomagnetic fields on thunderclouds, calculation of the forces (geomagnetic force, electric force, and force of gravity) is presented based on three amounts of the observed charges on hydrometeors.

As it is aimed to compare the electric force with the geomagnetic force in thunderclouds, the other forces (e.g., pressure gradient force, apparent Coriolis force, friction force, and apparent centrifugal force) are neglected in this study (and just the force of gravity is considered). Table 1 shows the calculation of forces based on three amounts of the observed charges on hydrometeors. In reference [13], tiny charged water droplets (from 0.01 µm to 1 µm in diameter) with charges in the range of: 9.8×10^{-18} to 2.5×10^{-14} Coulombs were considered while in this study, the electrified hydrometeors with radiuses from 10 µm to 1000 µm and charges of about 10^{-15} to 10^{-10} Coulombs are considered. The hydrometeors' masses are calculated based on the water droplet density (for ice crystal, the density is different).

Table 1. Calculation of the forces (geomagnetic force, electric force, and force of gravity) exerted on the charged hydrometeors in thunderclouds.

Parameters and Forces, (Unit), [Symbol] \ Reference of observed charges on particles	[55]	[5]	[5, 56]
Radius, (µm)	10	100	1000
Charge, (C), [q]	10^{-15}	10^{-13}	10^{-10}
Mass, (kg)$^{(\text{Note 1})}$, [m]	4.19×10^{-12}	4.19×10^{-9}	4.19×10^{-6}
$F_1 = E \cdot q$, (N) $(E_{fair\ weather} \approx 10^2\ \text{V m}^{-1})$	10^{-13}	10^{-11}	10^{-8}
$F_2 = E \cdot q$, (N) $(E_{thundercloud} = 10^4 \sim 10^6\ \text{V m}^{-1})$	$10^{-11} \sim 10^{-9}$	$10^{-9} \sim 10^{-7}$	$10^{-6} \sim 10^{-4}$
$F_3 = m \cdot g$, (N)	4.11×10^{-11}	4.11×10^{-8}	4.11×10^{-5}
$F_4 = q \cdot (v \times B)^{(\text{Note 2})}$, (N)	1.8×10^{-18}	1.8×10^{-16}	1.8×10^{-13}

Note 1: The masses are calculated based on water droplet density (and the density of ice crystal is different).
Note 2: $B_{(geomagnetic\ field)} = 6 \times 10^{-5}$ (T); Hydrometeor's velocity: $v = 30\,(\text{m s}^{-1})$.

It is clear that the electric force and the force of gravity approximately have the same orders, and they are much stronger than the geomagnetic force (at least 5 orders). In fact, the calculations presented in Table 1 confirm that the electric force and the force of gravity are salient, and the geomagnetic force is negligible in the vertical direction. It should be noted that the increment or decrement of the geomagnetic force depend on both the location (elevation, latitude, and longitude) and the velocity of charged hydrometeors.

It is an important point that the force of gravity is in the vertical direction ($\vec{z}$), but the electric force and the geomagnetic force could be in any direction ($\vec{x}, \vec{y}, \vec{z}$), and the directions of forces are not considered in Table 1 (although in fair weather conditions the electric force is just in vertical direction, but in thunderclouds there could be horizontal electric fields generated from horizontal opposite charge layers). Therefore, the effect of horizontal geomagnetic force (the combination of north/southward and east/westward components of the geomagnetic force) acting on the electrified hydrometeors could not be ignored in horizontal direction. All in all, the electric force and the force of gravity are much stronger than the geomagnetic force in vertical direction, and the electric force and geomagnetic force could not be ignored in horizontal direction.

In general, as a comparison between the electric force and geomagnetic force, it could be concluded that the electric force (in both of fair weather and thunderstorm conditions) plays a remarkable (more

important and impressive) role in the troposphere rather than the geomagnetic force and could strongly influence the formation of the thunderclouds' charge structure.

3.2. Effects of the Geomagnetic Field on the Electrical Properties of Thunderstorms

In this subsection of the study, some regions from five continents are selected in order to analyze the relation between the maps of the geomagnetic field (extracted from IGRF model) and the mean annual maps of both lightning activity and thunder day events (which are acquired from satellite-based/ground-based data and reports).

3.2.1. Africa

First, using the data from reference [51], the average level of lightning activity throughout the year (Flashes km^{-2} yr^{-1}) for 48 regions in Africa are compared with the geomagnetic field components, and the correlation coefficients are extracted.

Table 2 shows the correlation coefficients between the geomagnetic field components and the mean annual lightning flash rate data.

Table 2. Correlation between the geomagnetic field components (extracted from IGRF model) and the mean annual lightning flash rate (km^{-2} yr^{-1}) for 48 regions of Africa (from [51]).

Parameters (mean annual lightning and geomagnetic field)	Correlation Coefficient
Mean annual lightning flash rate & D (Declination)	−0.044
Mean annual lightning flash rate & I (Inclination)	−0.42264
Mean annual lightning flash rate & B_x (Northward geomagnetic field)	−0.03964
Mean annual lightning flash rate & B_y (Eastward geomagnetic field)	−0.12046
Mean annual lightning flash rate & B_z (Downward geomagnetic field)	−0.50379
Mean annual lightning flash rate & B_H (Horizontal geomagnetic field)	−0.0413
Mean annual lightning flash rate & B_T (Total geomagnetic field)	−0.45792

The results reveal good correlations between (the Downward, Total, and Inclination components of) the geomagnetic field and the mean annual lightning activity data in Africa (the absolute value of the correlation coefficients are from 0.4 to 0.5 for these parameters). The reverse relation between lightning activity and total geomagnetic field could be reported.

The Tropical Rainfall Measuring Mission (TRMM) Lightning Imaging Sensor (LIS) collected the observations of lightning in the global tropics and subtropics (roughly 38°S to 38°N). This space-based instrument has been used to detect the distribution and variability of total lightning [52]. The TRMM LIS operated successfully for over 17 years, from launch in December 1997 until April 2015. The satellite-based lightning data (from TRMM LIS) of Africa, for the regions between 35°S (−35) and 35°N (+35) latitudes; 20°W (−20) and 50°E (+50) longitudes, are extracted and compared with the total geomagnetic field. A comparison between the lightning density map (Fig. 1(b)) and the simulation results of the total geomagnetic field (Fig. 1(a)) in Africa reveals that approximately, regions with higher geomagnetic field almost have lower lightning density (which conform to the results obtained from Table 2 for the total geomagnetic field).

3.2.2. America

First, the satellite-based lightning data are considered so that these data cover the regions between 38°S (−38) and 38°N (+38) latitudes; 125°W (−125) and 35°W (−35) longitudes. Using the spatial distribution of the total geomagnetic field (Fig. 2(a)) which is extracted from IGRF model, a comparison is made between this map and the map of satellite-based lightning data (Fig. 2(b)) in America which shows that regions with lower geomagnetic field almost have higher lightning density.

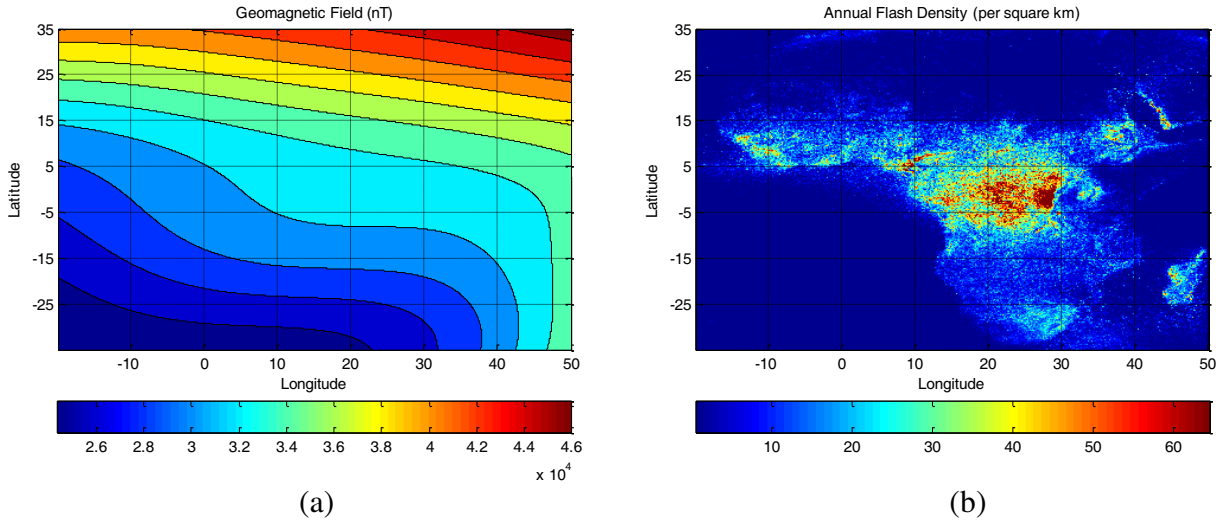

Figure 1. A comparison between (a) map of the total geomagnetic field (extracted from IGRF model) and (b) the annual lightning density map in Africa acquired from satellite-based lightning data (from TRMM LIS); the horizontal axis shows the longitude (degree) and the vertical axis depicts the latitude (degree).

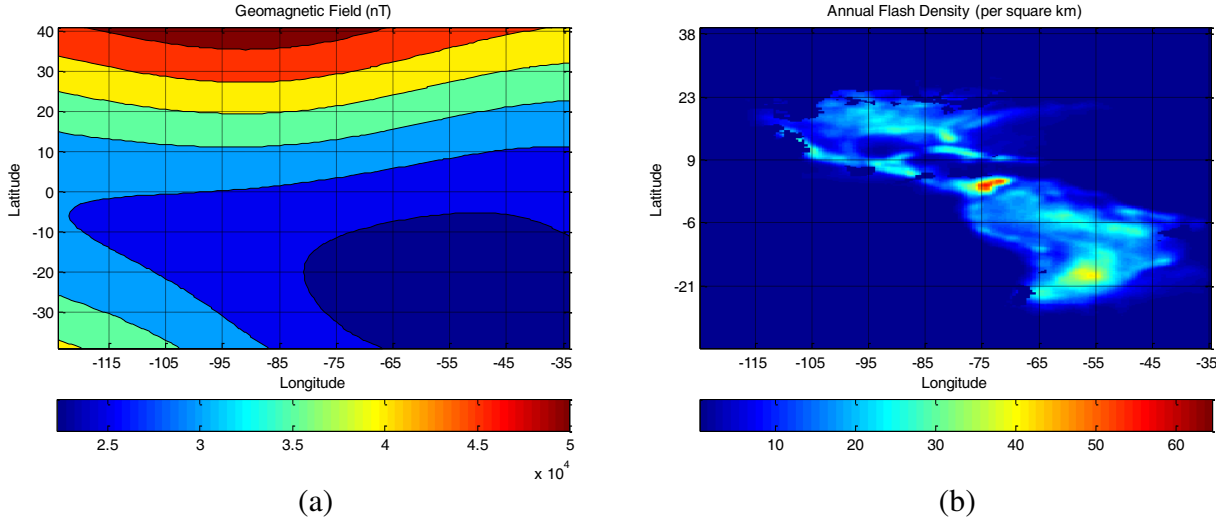

Figure 2. A comparison between (a) the map of total geomagnetic field (extracted from IGRF model) and (b) the annual lightning density map in America acquired from satellite-based lightning data (from TRMM LIS); the horizontal axis shows the longitude (degree) and the vertical axis depicts the latitude (degree).

As the data of TRMM LIS have a restriction of being bounded between 38°S (−38) and 38°N (+38) latitudes, it is not possible to consider the northern high latitudes (regions with latitudes more than 38°N) in America for the comparison which is made in this subsection.

Second, the thunder days' map (the average annual numbers of thunder events) of USA is considered in order to find some evidences for the relation between the total geomagnetic field and the thunderstorm activity (for the regions between 23°N (+23) and 50°N (+50) latitudes; 120°W (−120) and 50°W (−50) longitudes). The map of average annual number of thunder events in USA is adapted from reference [1].

A comparison between the thunder days' map (Fig. 3(b)) and the map of the total geomagnetic field (Fig. 3(a)) in the USA reveals that regions with lower total geomagnetic field almost have higher density of thunder days.

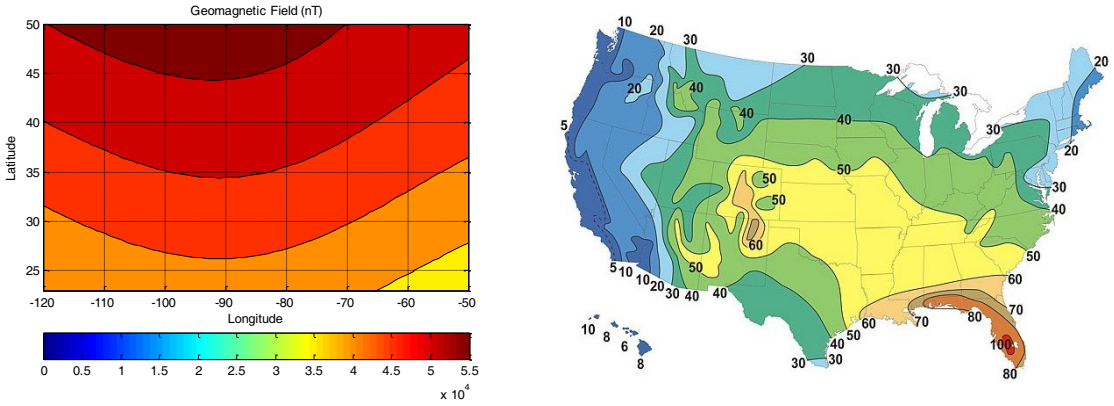

Figure 3. A comparison between (a) the map of total geomagnetic field (extracted from IGRF model) and (b) the map of average annual numbers of thunder events of USA (adapted from [1]); the horizontal axis shows the longitude (degree) and the vertical axis depicts the latitude (degree).

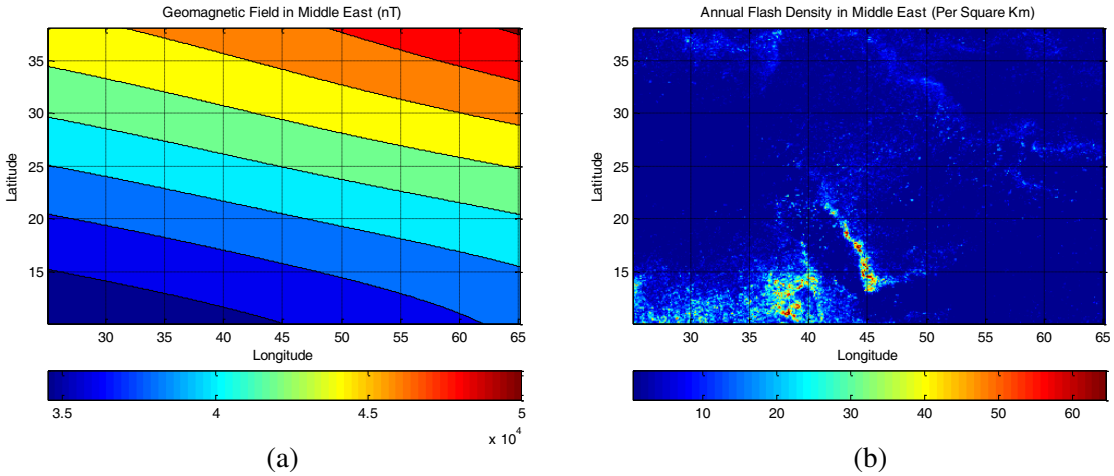

Figure 4. A comparison between (a) the map of total geomagnetic field (extracted from IGRF model) and (b) the lightning density map in Middle East acquired from satellite-based lightning data (from TRMM LIS); the horizontal axis shows the longitude (degree) and the vertical axis depicts the latitude (degree).

3.2.3. Asia

The satellite-based lightning data have been extracted from TRMM LIS for Middle East (the regions between 10°N (+10) and 38°N (+38) latitudes; 24°E (+24) and 64°E (+64) longitudes) in order to investigate the relation between the total geomagnetic field and the lightning data.

A comparison between the satellite-based lightning data (Fig. 4(b)) for Middle East and the total geomagnetic field (Fig. 4(a)), which is acquired from IGRF model, reveals that regions with lower total geomagnetic field almost have higher lightning density.

3.2.4. Australia

The geomagnetic field components in Australia are extracted from IGRF model. First, it is intended to compare the data of the geomagnetic field components with the data of the mean annual lightning activity and thunder day events. The values of the average annual CG flash density (N_g), obtained by ground-based lightning detection instruments, total flash density (N_t), and thunder days (T_d), obtained

by NASA satellite-based instruments, in 39 locations of Australia are derived from reference [53]. The data of N_g, N_t, and T_d for 39 locations of Australia are compared with the geomagnetic field components, and the correlation coefficients are extracted. The second column of Table 3 shows the correlation coefficients between the geomagnetic field components and the CG lightning (N_g) activity data. The results reveal good correlations between (the Northward, Downward, Horizontal, Total, and Inclination components of) the geomagnetic field and the N_g in Australia (the absolute value of the correlation coefficient coefficients are from 0.58 to 0.6 for these parameters). Moreover, the third and fourth columns of Table 3 show the correlation coefficients between the geomagnetic field components and both total lightning (N_t) activity and thunder day events (T_d). Approximately, the same results (as the second column) could be obtained from the comparison between these data. However, it should be noted that there are stronger relations between the geomagnetic field components and the data of thunder days (T_d).

Table 3. Correlation coefficients of the geomagnetic field components (extracted from IGRF model) with both lightning activity and thunder days data for 39 locations of Australia (derived from [53]).

LIGHTNING AND THUNDER DAYS / GEOMAGNETIC FIELD COMPONENTS	**CLOUD TO GROUND LIGHTNING (N_g)**	**TOTAL LIGHTNING (N_t)**	**THUNDER DAYS (T_d)**
B_x (Northward)	0.584423	0.537543	0.645302
B_y (Eastward)	0.108966	0.256888	0.127181
B_z (Downward)	0.600571	0.556216	0.671563
B_H (Horizontal)	0.589095	0.550634	0.65073
B_T (Total)	−0.58116	−0.55045	−0.65024
D (Declination)	0.017919	0.1608	0.023816
I (Inclination)	0.6082	0.556341	0.679544

Second, the spatial distribution of the total geomagnetic field is compared with the map of the average annual numbers of thunder events (as derived from [53]) in Australia (the regions between 38°S (−38) and 10°S (−10) latitudes; 115°E (+115) and 155°E (+155) longitudes). A comparison between the thunder days' map (Fig. 5(b)) and the simulation results of the total geomagnetic field (Fig. 5(a)) reveals that regions with lower total geomagnetic field almost have higher density of thunder days.

Third, the satellite-based lightning (Fig. 6(b)) data (from TRMM LIS) for the regions between 38°S (−38) and 10°S (−10) latitudes; 110°E (+110) and 160°E (+160) longitudes are extracted and compared with the total geomagnetic field (Fig. 6(a)). A comparison between the lightning density map (Fig. 6(b)) and the high resolution simulation results of the total geomagnetic field (Fig. 6(a)) in Australia reveals that regions with lower total geomagnetic field almost have higher lightning density.

3.2.5. Europe

In this subsection of the study, as the satellite-based lightning data of TRMM LIS have a restriction of being bounded between 38°S (−38) and 38°N (+38) latitudes, it is not possible to consider the northern high latitudes (regions with latitudes more than 38°N) in Europe. Therefore, the lightning data of the Europe are derived from the Earth Networks Global Lightning Network (ENGLN), which monitors the combination of in-cloud and cloud-to-ground lightning strikes [54] over 100 countries with over 1,800 sensors. The data include the in-cloud lightning, cloud-to-ground lightning, total lightning, and thunder days for 34 regions in Europe during 2019. The first 13 countries with highest amounts of lightning activity in Europe are selected, and the relations between the geomagnetic field components and both thunder days and lightning activity are investigated for these countries; the correlation coefficients are extracted. The second column of Table 4 shows the correlation coefficients between the geomagnetic field components and the thunder days' data. Moreover, the third column of Table 4 is dedicated to the

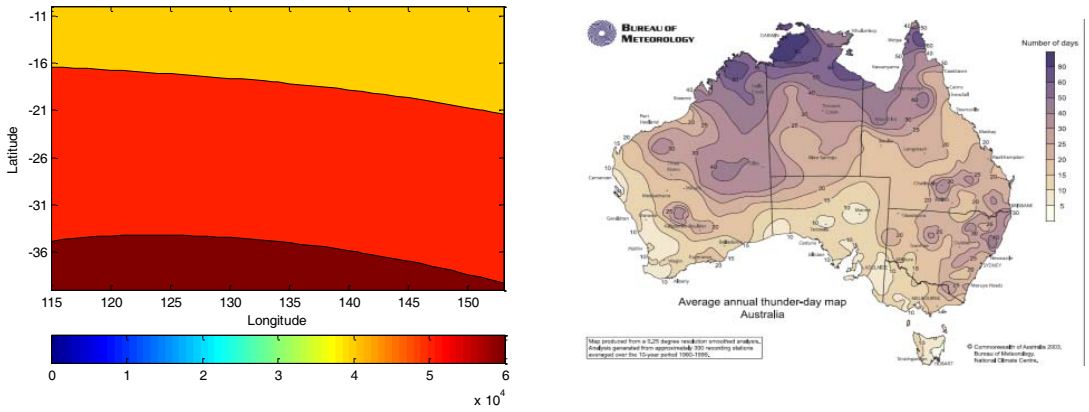

(a) (b)

Figure 5. (a) Total geomagnetic field (nT), extracted from IGRF model for Australia; (b) Values of the average annual Thunder days (T_d), derived from [53] for Australia.

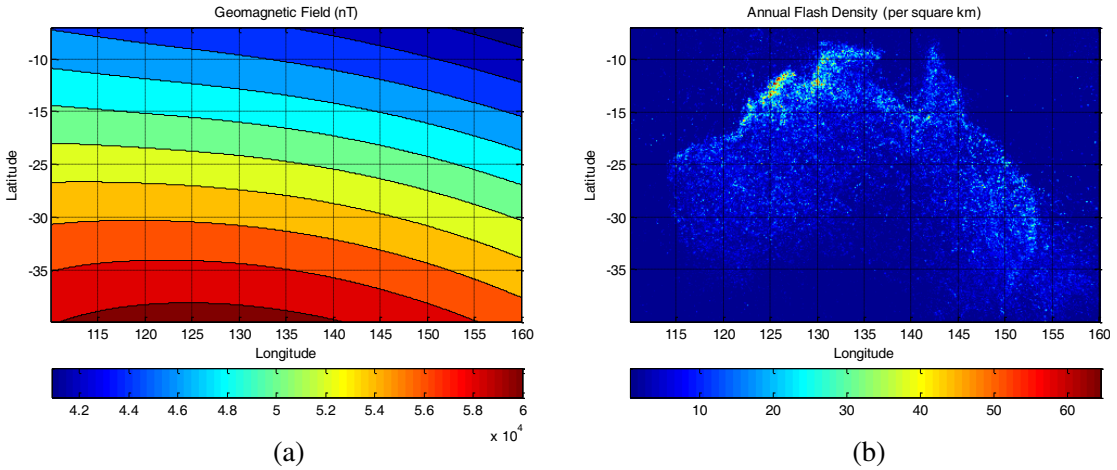

(a) (b)

Figure 6. A comparison between (a) the map of total geomagnetic field (extracted from IGRF model) and (b) the lightning density map in Australia acquired from satellite-based lightning data (from TRMM LIS); the horizontal axis shows the longitude (degree) and the vertical axis depicts the latitude (degree).

correlation coefficients between the geomagnetic field components and the total lightning activity data. The results reveal a good (reverse) correlation of the total geomagnetic field with the thunder day' data in Europe (the absolute value of the correlation is about 0.42).

With regard to the calculated correlation coefficients (in Table 2, Table 3, and Table 4), it could be concluded that in the hotspot regions, the thunderstorms' electrical properties are inversely correlated with the total geomagnetic field. It should be noted that the thunderstorms' electrical properties in some regions might (at the same time) be correlated with I, B_x, B_z, and B_H. This is probably influenced by the relations between the components of the geomagnetic field (as the total geomagnetic field is the net of northward, eastward, and downward components of the geomagnetic field and also the inclination and horizontal components of the geomagnetic field are related to the total geomagnetic field). Moreover, it is an important point that the sign of the total and the horizontal geomagnetic field in all latitudes and longitudes are positive, but the sign of the inclination, declination, and (northward, eastward, and downward) components of the geomagnetic field depends on the location. For instance, the sign of the correlation between the downward component of the geomagnetic field and the thunderstorms' electrical properties is positive in Australia and negative in Africa and Europe. All in all, the total geomagnetic field in most of the hotspots on the Earth has an inverse relation with thunderstorms' electrical activities.

Table 4. Correlation between the geomagnetic field components and thunderstorm (lightning) activity data for the first 13 countries with highest amounts of lightning activity in Europe during 2019.

LIGHTNING AND THUNDER DAYS GEOMAGNETIC FIELD COMPONENTS	Thunder Days	Total Lightning
B_T (Total)	−0.41707973	−0.33455215
B_H (Horizontal)	0.426575187	0.465433061
B_z (Downward)	−0.437092269	−0.413718252
B_y (Eastward)	−0.256986987	0.009548218
B_x (Northward)	0.430869297	0.461177915
I (Inclination)	−0.432599283	−0.455626069
D (Declination)	−0.38822674	−0.104962392

3.2.6. Worldwide

First, the satellite-based lightning data of TRMM LIS (which covers the regions between 38°S (−38) and 38°N (+38) latitudes; 180°W (−180) and 180°E (+180) longitudes) are considered in this section. Moreover, the geomagnetic field values are extracted from IGRF model in order to show the relation between the geomagnetic field and the global average annual lightning distribution.

A comparison between the map of the total geomagnetic field (Fig. 7(a)) and the map of the global lightning distribution (Fig. 7(b)) shows that the regions with lower amount of total geomagnetic field almost have higher lightning activity.

Furthermore, the correlation coefficients between the total geomagnetic field and the global mean annual lightning activity are extracted. With regard to the TRMM LIS data, the latitude accuracy is 0.1° for latitudes from 38°S to 38°N; therefore, 760 rows will be generated in lightning activity matrix. The longitude accuracy is 0.1° for longitudes from 180°W to 180°E; therefore, 3600 columns will be generated in lightning activity matrix. In this study, the global mean annual lightning activity matrix and the total geomagnetic field matrix have the same dimensions of 760 × 3600.

The first row of the lightning activity matrix is compared with each row of the total geomagnetic field matrix, and these values of correlation coefficients establish the first row of the horizontal correlation matrix. In this way, a matrix with the dimensions of 760 × 760 will result which is illustrated in Fig. 8.

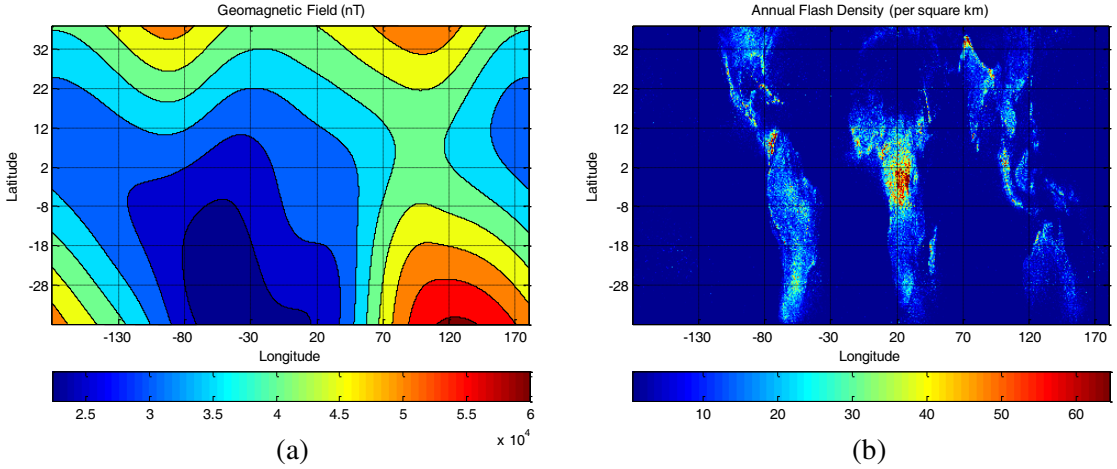

Figure 7. A comparison between (a) the map of total geomagnetic field (extracted from IGRF model) and (b) the global lightning density map acquired from satellite-based lightning data (from TRMM LIS); the horizontal axis shows the longitude (degree) and the vertical axis depicts the latitude (degree).

This figure shows that in regions with latitudes from 38°S to 12°N and from 33°N to 38°N the reverse relation between the lightning activity and the total geomagnetic field is stronger. This should be noted that almost the highest lightning activity occurs in these latitudes.

The first column of the lightning activity matrix is compared with each column of the total geomagnetic field matrix, and these values of correlation coefficients establish the first column of the vertical correlation matrix. In this way, a matrix with the dimensions of 3600×3600 will result which is illustrated in Fig. 9.

This figure shows that in regions with longitudes from 80°W to 40°W, from 15°W to 40°E, and from 75°E to 120°E, the reverse relation between the lightning activity and the total geomagnetic field is stronger. It should be noted that approximately the highest lightning activity occurs in these longitudes.

Second, the global thunder days' map (the average annual numbers of thunder events) is considered (Fig. 10(b)) in order to find some evidences for the relation between the total geomagnetic field (Fig. 10(a)) and the thunderstorm activity (for the regions between 80°S (−80) and 80°N (+80) latitudes; 180°W (−180) and 180°E (+180) longitudes). A comparison between these two maps shows that the regions with lower amount of total geomagnetic field almost have higher thunderstorm activity.

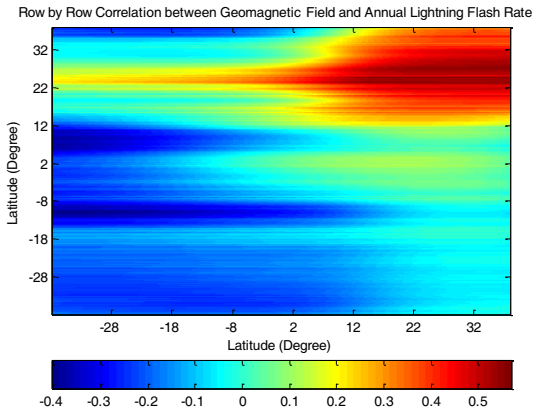

Figure 8. The horizontal correlation matrix which is established from the correlation between each row of the lightning activity matrix (obtained from the satellite-based lightning data) and each row of the total geomagnetic field matrix (extracted from IGRF model).

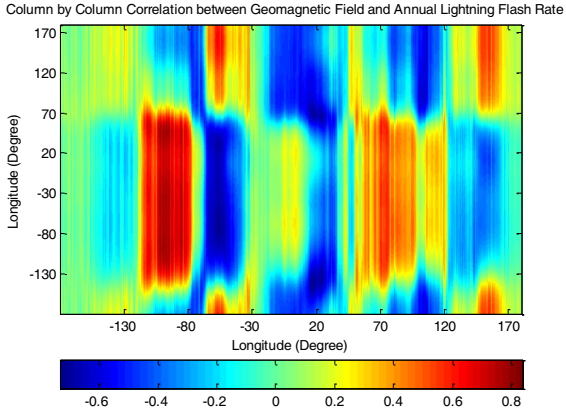

Figure 9. The vertical correlation matrix which is established from the correlation between each column of the lightning activity matrix (obtained from the satellite-based lightning data) and each column of the total geomagnetic field matrix (extracted from IGRF model).

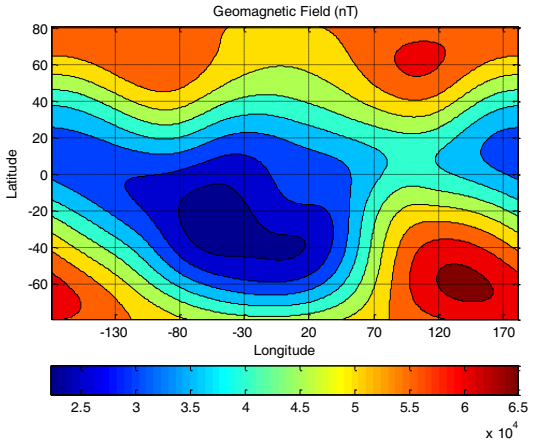

(a)

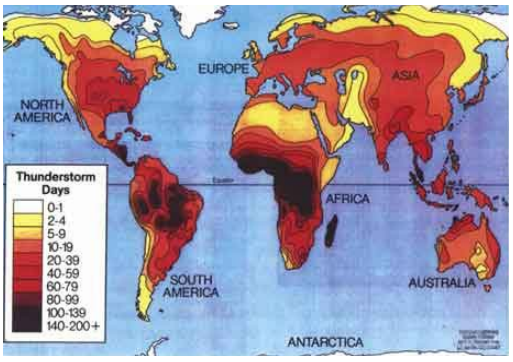

(b)

Figure 10. A comparison between (a) the map of total geomagnetic field (extracted from IGRF model) and (b) the map of average global annual numbers of thunder events.

4. CONCLUSION

In the present study, a comparison has been made between the electric and geomagnetic forces acting on the electrified hydrometeors in thunderstorms. First, the calculations showed that the intensity of the electric force (in both of fair weather and thunderstorm conditions) plays a more impressive role in troposphere than the geomagnetic force and could remarkably influence the formation of the thunderclouds' charge structure.

Moreover, as the electric field increases in thunderstorm conditions (regarding the dependence of the induction mechanism of cloud electrification to the electric field), the increased electric field strengthens the induction mechanism of cloud electrification and influences the electrical properties of thunderstorm. It should be emphasized that while specifying the geomagnetic field and the electric field as important factors which could influence the thunderclouds' properties, we do not lessen the contribution of other factors (e.g., the pressure gradient force and the Coriolis force).

Second, through drawing a comparison between the spatial distribution of the geomagnetic field (obtained from IGRF model) and the mean annual spatial distribution of both lightning activity and thunder day events (acquired from satellite-based/ground-based data and reports), an inverse relation between the geomagnetic field and both annual lightning density and thunder day events in most of the hot spots on the Earth has been revealed.

Furthermore, the correlation coefficients of the global geomagnetic field and the global mean annual lightning activity are extracted (in the global tropics and subtropics). Analysis of both horizontal and vertical correlation matrices showed that approximately in latitudes and longitudes with high lightning density, the reverse relation between the average annual lightning activity and the total geomagnetic field is stronger. Moreover, a comparison between the global annual thunder days' map and the map of geomagnetic field revealed an inverse relation between these two maps.

All in all, based on the results of this study, two main conclusions could be reported; first, there is an inverse relation between the spatial distribution of the total geomagnetic field and the mean annual spatial distribution of both lightning activity and thunder day events; second, the influence of the electric force on thunderclouds' electrical properties is more powerful than the effect of the geomagnetic force.

5. DECLARATION OF INTERESTS

The authors declare that they have no known competing financial interests or personal relationships that could have appeared to influence the work reported in this paper.

6. FUNDING

The research has no sources of funding.

ACKNOWLEDGMENT

We thank the *NASA Global Hydrology Resource Center DAAC* and the *Earth Networks* for data that have been provided. We would also like to show our gratitude to the *International Association of Geomagnetism and Aeronomy (IAGA)* for sharing their data.

We would like to thank the editor and two anonymous reviewers for their insightful comments and constructive suggestions, which significantly helped us to improve the manuscript quality.

REFERENCES

1. Rakov, V. A. and M. A. Uman, *Lightning: Physics and Effects*, Cambridge University Press, 2003, https://doi.org/10.1017/CBO9781107340886.
2. Marshall, T., S. Bandara, N. Karunarathne, S. Karunarathne, I. Kolmasova, R. Siedlecki, and M. Stolzenburg, "A study of lightning flash initiation prior to the first initial breakdown pulse," *Atmospheric Research*, Vol. 217, 10–23, 2019, https://doi.org/10.1016/j.atmosres.2018.10.013.

3. Berkopec, A., "Fast particles as initiators of stepped leaders in CG and IC lightnings," *Journal of Electrostatics*, Vol. 70, 462–467, 2012, https://doi.org/10.1016/j.elstat.2012.07.001.
4. Gao, X., N. Liu, F. Shi, and H. K. Rassoul, "Streamer discharge initiation from an isolated spherical hydrometeor at subbreakdown condition," *Journal of Electrostatics*, Vol. 106, 103457, 2020, https://doi.org/10.1016/j.elstat.2020.103457.
5. Latham, J., "The electrification of thunderstorms," *Quarterly Journal of the Royal Meteorological Society*, Vol. 107, 277–298, 1981, https://doi.org/10.1002/qj.49710745202.
6. Rycroft, M. J., A. Odzimek, N. F. Arnold, M. Füllekrug, A. Kułak, and T. Neubert, "New model simulations of the global atmospheric electric circuit driven by thunderstorms and electrified shower clouds: The roles of lightning and sprites," *Journal of Atmospheric and Solar-Terrestrial Physics*, Vol. 69, 2485–2509, 2007, https://doi.org/10.1016/j.jastp.2007.09.004.
7. Liu, C., E. R. Williams, E. J. Zipser, and G. Burns, "Diurnal variations of global thunderstorms and electrified shower clouds and their contribution to the global electrical circuit," *Journal of the Atmospheric Sciences*, Vol. 67, 309–323, 2010, https://doi.org/10.1175/2009jas3248.1.
8. Harrison, G., "The cloud chamber and CTR Wilson's legacy to atmospheric science," *Weather*, Vol. 66, 276–279, 2011, https://doi.org/10.1002/wea.830.
9. Nicoll, K., "Space weather influences on atmospheric electricity," *Weather*, Vol. 69, 238–241, 2014, https://doi.org/10.1002/wea.2323.
10. Mangla, B., D. Sharma, and A. Rajput, "Ion density variation at upper ionosphere during thunderstorm," *Advances in Space Research*, Vol. 59, 1189–1199, 2017, https://doi.org/10.1016/j.asr.2016.11.039.
11. Burns, G., A. Frank-Kamenetsky, B. Tinsley, W. French, P. Grigioni, G. Camporeale, and E. Bering, "Atmospheric global circuit variations from Vostok and Concordia electric field measurements," *Journal of the Atmospheric Sciences*, Vol. 74, 783–800, 2017, https://doi.org/10.1175/jas-d-16-0159.1.
12. Nina, A., M. Radovanović, B. Milovanović, A. Kovačević, J. Bajčetić, and L. Č, Popović, "Low ionospheric reactions on tropical depressions prior hurricanes," *Advances in Space Research*, Vol. 60, 1866–1877, 2017, https://doi.org/10.1016/j.asr.2017.05.024.
13. Dehel, T. F., M. Dickinson, F. Lorge, and R. Startzel, Jr., "Electric field and Lorentz force contribution to atmospheric vortex phenomena," *Journal of Electrostatics*, Vol. 65, 631–638, 2007, https://doi.org/10.1016/j.elstat.2007.04.001.
14. Schultz, D. M. and R. J. Vavrek, "An overview of thundersnow," *Weather*, Vol. 64, 274–277, 2009, https://doi.org/10.1002/wea.376.
15. Takahashi, T., T. Tajiri, and Y. Sonoi, "Charges on graupel and snow crystals and the electrical structure of winter thunderstorms," *Journal of the Atmospheric Sciences*, Vol. 56, 1561–1578, 1999, https://doi.org/10.1175/1520-0469(1999)056%3C1561:cogasc%3E2.0.co;2.
16. Thébault, E., C. C. Finlay, C. D. Beggan, P. Alken, J. Aubert, O. Barrois, F. Bertrand, T. Bondar, A. Boness, and L. Brocco, "International geomagnetic reference field: The 12th generation," *Earth, Planets and Space*, Vol. 67, 79, 2015, https://doi.org/10.1186/s40623-015-0228-9.
17. Macmillan, S., "Earth's magnetic field, Geophysics and Geochemistry, Encyclopedia of Life Support Systems (EOLSS)," *Developed under the Auspices of the UNESCO*, Eolss Publishers, Oxford, UK, 2006, https://www.eolss.net/sample-chapters/C01/E6-16-04-01.pdf.
18. Stolzenburg, M., W. D. Rust, B. F. Smull, and T. C. Marshall, "Electrical structure in thunderstorm convective regions: 1. Mesoscale convective systems," *Journal of Geophysical Research: Atmospheres*, Vol. 103, 14059–14078, 1998, https://doi.org/10.1029/97jd03546.
19. Pineda, N., T. Rigo, J. Montanyà, and O. A. van der Velde, "Charge structure analysis of a severe hailstorm with predominantly positive cloud-to-ground lightning," *Atmospheric Research*, Vol. 178, 31–44, 2016, https://doi.org/10.1016/j.atmosres.2016.03.010.
20. Molinari, J., D. Vollaro, and K. L. Corbosiero, "Tropical cyclone formation in a sheared environment: A case study," *Journal of the Atmospheric Sciences*, Vol. 61, 2493–2509, 2004, https://doi.org/10.1175/jas3291.1.

21. Wiens, K. C., S. A. Rutledge, and S. A. Tessendorf, "The 29 June 2000 supercell observed during STEPS. Part II: Lightning and charge structure," *Journal of the Atmospheric Sciences*, Vol. 62, 4151–4177, 2005, https://doi.org/10.1175/jas3615.1.
22. Barthe, C., T. Hoarau, and C. Bovalo, "Cloud electrification and lightning activity in a tropical cyclone-like vortex," *Atmospheric Research*, Vol. 180, 297–309, 2016, https://doi.org/10.1016/j.atmosres.2016.05.023.
23. Ahmad, A. and M. Ghosh, "Variability of lightning activity over India on ENSO time scales," *Advances in Space Research*, Vol. 60, 2379–2388, 2017, https://doi.org/10.1016/j.asr.2017.09.018.
24. Matthews, J., M. Wright, D. Clarke, E. Morley, H. Silva, A. Bennett, D. Robert, and D. Shallcross, "Urban and rural measurements of atmospheric potential gradient," *Journal of Electrostatics*, Vol. 97, 42–50, 2019, https://doi.org/10.1016/j.elstat.2018.11.006.
25. Nicoll, K., "Measurements of atmospheric electricity aloft," *Surveys in Geophysics*, Vol. 33, 991–1057, 2012, https://doi.org/10.1007/s10712-012-9188-9.
26. Falconer, R. E., "A correlation between atmospheric electrical activity and the jet stream," *General Electric Co Schenectady*, NY, 1953, https://apps.dtic.mil/dtic/tr/fulltext/u2/015500.pdf.
27. Saunders, C., "Charge separation mechanisms in clouds," *Space Science Reviews*, Vol. 137, 335, 2008, https://doi.org/10.1007/978-0-387-87664-1_22.
28. Krasilnikov, E. Y., "Electromagnetohydrodynamic nature of tropical cyclones, hurricanes, and tornadoes," *Journal of Geophysical Research: Atmospheres* Vol. 102, 13571–13580, 1997, https://doi.org/10.1029/97jd00146.
29. Artekha, S. and A. Belyan, "On the role of electromagnetic phenomena in some atmospheric processes," *Nonlinear Processes in Geophysics*, Vol. 20, 293–304, 2013, https://doi.org/10.5194/npg-20-293-2013.
30. Toth III, J. R., S. Rajupet, H. Squire, B. Volbers, J. Zhou, L. Xie, R. M. Sankaran, and D. J. Lacks, "Electrostatic forces alter particle size distributions in atmospheric dust," *Atmospheric Chemistry & Physics*, Vol. 20, 3181–3190, 2020, https://doi.org/10.5194/acp-20-3181-2020.
31. Pang, X. F., "The experimental evidences of the magnetism of water by magnetic-field treatment," *IEEE Transactions on Applied Superconductivity*, Vol. 24, 1–6, 2014, https://doi.org/10.1109/tasc.2014.2340455.
32. Cai, R., H. Yang, J. He, and W. Zhu, "The effects of magnetic fields on water molecular hydrogen bonds," *Journal of Molecular Structure*, Vol. 938, 15–19, 2009, https://doi.org/10.1016/j.molstruc.2009.08.037.
33. Pang, X.-F. and G.-F. Shen, "The changes of physical properties of water arising from the magnetic field and its mechanism," *Modern Physics Letters B*, Vol. 27, 1350228:1-9, 2013, https://doi.org/10.1142/s021798491350228x.
34. Semikhina, L. and V. Kiselev, "Effect of weak magnetic fields on the properties of water and ice," *Soviet Physics Journal*, Vol. 31, 351–354, 1988, https://doi.org/10.1007/bf01243721.
35. Mohri, K. and M. Fukushima, "Gradual decreasing characteristics and temperature stability of electric resistivity in water triggered with milligauss AC field," *IEEE Transactions on Magnetics*, Vol. 38, 3353–3355, 2002, https://doi.org/10.1109/tmag.2002.802307.
36. Saunders, C., "Charge separation mechanisms in clouds," *Space Science Reviews*, Vol. 137, 335–353, 2008, https://doi.org/10.1007/s11214-008-9345-0.
37. Takahashi, T., S. Sugimoto, T. Kawano, and K. Suzuki, "Riming electrification in Hokuriku winter clouds and comparison with laboratory observations," *Journal of the Atmospheric Sciences*, Vol. 74, 431–447, 2017, https://doi.org/10.1175/jas-d-16-0154.1.
38. Emersic, C. and C. Saunders, "Further laboratory investigations into the relative diffusional growth rate theory of thunderstorm electrification," *Atmospheric Research*, Vol. 98, 327–340, 2010, https://doi.org/10.1016/j.atmosres.2010.07.011.
39. Lamb, H. H., *Climate: Present, Past and Future (Routledge Revivals): Volume 2: Climatic History and the Future, Routledge*, 2013, https://doi.org/10.4324/9780203804315.

40. King, J., "Weather and the Earth's magnetic field," *Nature*, Vol. 247, 131–134, 1974, https://doi.org/10.1038/247131a0.
41. King, J. and D. Willis, "Magnetometeorology: Relationships between the weather and Earth's magnetic field," NASA, 1975, https://ntrs.nasa.gov/search.jsp?R=19760007443.
42. Svensmark, H. and E. Friis-Christensen, "Variation of cosmic ray flux and global cloud coverage — A missing link in solar-climate relationships," *Journal of Atmospheric and Solar-Terrestrial Physics*, Vol. 59, 1225–1232, 1997, https://doi.org/10.1016/s1364-6826(97)00001-1.
43. Courtillot, V., Y. Gallet, J.-L. Le Mouël, F. Fluteau, and A. Genevey, "Are there connections between the Earth's magnetic field and climate?," *Earth and Planetary Science Letters*, Vol. 253, 328–339, 2007, http://dx.doi.org/10.1016/j.epsl.2006.10.032.
44. Knudsen, M. F. and P. Riisager, "Is there a link between Earth's magnetic field and low-latitude precipitation?," *Geology*, Vol. 37, 71–74, 2009, https://doi.org/10.1130/g25238a.1.
45. Anderson, R. Y., "Possible connection between surface winds, solar activity and the Earth's magnetic field," *Nature*, Vol. 358, 51–53, 1992, https://doi.org/10.1038/358051a0.
46. Schlegel, K., G. Diendorfer, S. Thern, and M. Schmidt, "Thunderstorms, lightning and solar activity — Middle Europe," *Journal of Atmospheric and Solar-Terrestrial Physics*, Vol. 63, 1705–1713, 2001, https://doi.org/10.1016/s1364-6826(01)00053-0.
47. Gurevich, A. V. and K. P. Zybin, "Runaway breakdown and the mysteries of lightning," *Phys. Today*, Vol. 58, 37–43, 2005, https://doi.org/10.1063/1.1995746.
48. Babich, L. P., E. I. Bochkov, J. R. Dwyer, and I. M. Kutsyk, "Numerical simulations of local thundercloud field enhancements caused by runaway avalanches seeded by cosmic rays and their role in lightning initiation," *Journal of Geophysical Research: Space Physics*, Vol. 117, 2012, https://doi.org/10.1029/2012ja017799.
49. Lindy, N., E. Benton, W. Beasley, and D. Petersen, "Energetic cosmic-ray secondary electron distribution at thunderstorm altitudes," *Journal of Atmospheric and Solar-Terrestrial Physics*, Vol. 179, 435–440, 2018, https://doi.org/10.1016/j.jastp.2018.10.003.
50. Jeon, J., S.-J. Noh, and D.-H. Lee, "Relationship between lightning and solar activity for recorded between CE 1392–1877 in Korea," *Journal of Atmospheric and Solar-Terrestrial Physics*, Vol. 172, 63–68, 2018, https://doi.org/10.1016/j.jastp.2018.03.020.
51. Collier, A. and A. Hughes, "A harmonic model for the temporal variation of lightning activity over Africa," *Journal of Geophysical Research: Atmospheres*, Vol. 116, 2011, https://doi.org/10.1029/2010JD014455.
52. Cecil, D. J., D. E. Buechler, and R. J. Blakeslee, "Gridded lightning climatology from TRMM-LIS and OTD: Dataset description," *Atmospheric Research*, Vol. 135, 404–414, 2014, https://dx.doi.org/10.5067/LIS/LIS-OTD/DATA311.
53. Kuleshov, Y., D. Mackerras, and M. Darveniza, "Spatial distribution and frequency of lightning activity and lightning flash density maps for Australia," *Journal of Geophysical Research: Atmospheres*, Vol. 111, 2006, https://doi.org/10.1029/2005JD006982.
54. Lapierre, J., M. Hoekzema, M. Stock, C. Merrill, and S. C. Thangaraj, "Earth networks lightning network and dangerous thunderstorm alerts," *2019 11th Asia-Pacific International Conference on Lightning (APL)*, 1–5, IEEE, 2019, https://doi.org/10.1109/APL.2019.8816032.
55. Kuettner, J. P., J. D. Sartor, and Z. Levin, "Thunderstorm electrification — Inductive or non-inductive?," *Journal of the Atmospheric Sciences*, Vol. 38, 2470–2484, 1981, https://doi.org/10.1175/1520-0469(1981)038%3C2470:teoni%3E2.0.co;2.
56. Christian, H., C. Holmes, J. Bullock, W. Gaskell, A. Illingworth, and J. Latham, "Airborne and ground-based studies of thunderstorms in the vicinity of Langmuir Laboratory," *Quarterly Journal of the Royal Meteorological Society*, Vol. 106, 159–174, 1980, https://doi.org/10.1002/qj.49710644711.